Octupole phonon model based on the shell model for octupole vibrational states

N. Yoshinaga,[1,*] K. Yanase,[1,†] K. Higashiyama,[2,‡] and E. Teruya[1,§]
[1]*Department of Physics, Saitama University, Saitama City 338-8570, Japan*
[2]*Department of Physics, Chiba Institute of Technology, Narashino, Chiba 275-0023, Japan*

(Received 3 September 2018; published 29 October 2018)

A model is proposed for a description of the octupole vibrational states based on the nuclear shell model. In this model, a one-octupole-phonon representing the collective octupole vibration across the magic core is introduced onto the shell-model states that are microscopically calculated within the valence nucleon space. With this model, a unified description is now possible for the pure shell-model states made by valence nucleons, and the octupole-phonon states excited on the shell-model states. The model is applied to various nuclei around the ^{208}Pb nucleus. Energy levels and electric octupole transition probabilities are well reproduced for both the pure shell-model states and the octupole vibrational states.

DOI: 10.1103/PhysRevC.98.044321

I. INTRODUCTION

Octupole correlations play an important role in determining the low-lying structure of nuclei throughout the periodic table [1,2]. Nuclei around the double-magic nucleus ^{208}Pb provides an ideal laboratory to study the concept of octupole-phonon vibrations in nuclear systems because the first excited 3^- states of these nuclei have long been interpreted as collective one-octupole-phonon states. In fact large electric octupole transition probabilities between low-lying 3^- states and the ground 0^+ states have been experimentally observed in ^{208}Pb [3,4], ^{206}Pb [5,6], and ^{210}Pb [7]. A high-spin alternating parity band was also discovered in ^{216}Rn [8]. Microscopically, they result from the long-range, octupole-octupole interaction between nucleons occupying pairs of orbitals with $\Delta j = 3$ and $\Delta l = 3$. One-octupole-phonon and multioctupole-phonon excitations around ^{208}Pb have been studied in theory by many authors [9–17].

The nuclear shell model is one of the most successful models in nuclear structure. In our previous studies [18–21], low-lying states in the mass number $A = 130$ and 200 regions were systematically reproduced in the nuclear shell model. The octupole-phonon states, which arise from one-particle one-hole excitations across the magic cores were excluded in the previous framework of the nuclear shell model, where the number of the shell-model configurations was limited due to the computational feasibility.

The octupole vibration and deformation are closely related to the parity (P) odd nuclear moments. The nuclear Schiff moments and the magnetic quadrupole moments can be largely enhanced in deformed nuclei, for example ^{225}Ra [22], ^{161}Dy, and ^{237}Np [23]. Moreover, an additional enhancement mechanism due to the coexistence of collective quadrupole and octupole modes was suggested, and the effect has been confirmed in RPA-based calculations [24,25]. Another enhancement mechanism of the CP violating interactions due to α-cluster structures is expected in light nuclei [26–28]. In spherical nuclei the nuclear Schiff moment of ^{129}Xe [29–31] and nuclear dipole moments of ^{129}Xe [32,33] and ^{199}Hg [34] are precisely calculated in the nuclear shell model.

In this paper the shell-model states and one-octupole-phonon states are unified by introducing an octupole phonon, which is helpful to identify the octupole vibrational states based on the shell-model configurations. The model is applied to various nuclei around the ^{208}Pb nucleus.

This paper is organized as follows. In Sec. II theoretical framework is given where the collective octupole phonon (f boson) is introduced. In Sec. III numerical results are given. Finally, a summary is given in Sec. IV.

II. THEORETICAL FRAMEWORK

A phenomenological model is introduced in this paper to describe collective octupole-phonon excitations based on the shell-model (SM) states. In this model a collective octupole-phonon (f boson) weakly couples with each shell-model state. The total Hamiltonian reads

$$\hat{H} = \hat{H}_{\rm SM} + \hat{H}_f + \hat{H}_{{\rm SM}-f}, \tag{1}$$

where $\hat{H}_{\rm SM}$ is the shell-model Hamiltonian for valence neutrons and protons. The explicit form of the shell-model Hamiltonian and the strengths of the interactions are given in Ref. [20] for the neutron number $N \leqslant 126$ and in Ref. [21] for $N > 126$. In these works, the shell-model configurations involve all the valence nucleons and all the single-particle orbitals in each one-major shell.

The f-boson one-body Hamiltonian is given as

$$\hat{H}_f = \varepsilon_f f^\dagger \cdot \tilde{f}, \tag{2}$$

*yoshinaga@phy.saitama-u.ac.jp
†yanase@nuclei.th.phy.saitama-u.ac.jp
‡koji.higashiyama@it-chiba.ac.jp
§teruya@nuclei.th.phy.saitama-u.ac.jp

where $f^\dagger$ and $\widetilde{f}_\mu = (-1)^{3-\mu} f_{-\mu}$ are the f-boson creation and annihilation operators, respectively, with angular momentum 3 and negative parity. As will be discussed in detail, the single f-boson energy ε_f is introduced as a phenomenological parameter.

The interaction between one f boson and each shell-model state is simply assumed to be a dipole-type with a coupling constant α:

$$\hat{H}_{\mathrm{SM}-f} = \alpha\, \boldsymbol{I}_{\mathrm{SM}} \cdot \boldsymbol{L}_f, \tag{3}$$

where $\boldsymbol{I}_{\mathrm{SM}}$ indicates the angular momentum in the valence space and $\boldsymbol{L}_f$ is the angular momentum of the f boson that is defined as

$$L_f^{(1)} = \sqrt{14}[f^\dagger \widetilde{f}]^{(1)}. \tag{4}$$

This dipole-type interaction represents the Coriolis force that does not admix the pure shell-model states with the one-octupole-phonon excited states. Then f-boson state coupled with each shell-model state is explicitly constructed as

$$\left|I_k^\pi; J\right\rangle_f = \left[|f\rangle \otimes \left|I_k^\pi\right\rangle_{\mathrm{SM}}\right]^{(J)}, \tag{5}$$

where $|I_k^\pi\rangle_{\mathrm{SM}}$ is the kth eigenstate with spin I and parity π of the shell-model Hamiltonian within the valence space. Here the shell-model states $|I_k^\pi\rangle_{\mathrm{SM}}$ are given by diagonalizing the shell-model Hamiltonian as

$$\hat{H}_{\mathrm{SM}}\left|I_k^\pi\right\rangle_{\mathrm{SM}} = E_{\mathrm{SM}}\left(I_k^\pi\right)\left|I_k^\pi\right\rangle_{\mathrm{SM}}. \tag{6}$$

The total angular momenta J of the f-boson state coupled with the shell-model I_k^π state are given by

$$J = |I-3|,\ |I-3|+1,\ \ldots,\ I+3. \tag{7}$$

It should be noted that the f-boson state coupled with the shell-model I_k^π state has the opposite parity to the corresponding shell-model state. The energy of the f-boson state coupled with the shell-model I_k^π state is given as

$$E_f\left(I_k^\pi; J\right) = E_{\mathrm{SM}}\left(I_k^\pi\right) + \varepsilon_f + \tfrac{1}{2}\alpha[J(J+1) - I(I+1) - 12]. \tag{8}$$

As for the single f-boson energies ε_f, the excitation energies of the 3_1^- states are adopted if they are experimentally known. Those values are $\varepsilon_f = 2.648$ and 1.870 MeV for ^{206,210}Pb, respectively, and $\varepsilon_f = 2.387$, 1.537, and 1.275 MeV for ^{210,212,214}Po, respectively. For other nuclei where any 3^- states are not observed, linearly optimized values with mass number A given in MeV as

$$\varepsilon_f = -0.121A + 27.3, \tag{9}$$

are employed. Here the neutron-closed, proton-closed, and deformed nuclei are excluded in the process of optimization.

Figure 1(a) shows the ratio $[R_{4/2} = E(4_1^+)/E(2_1^+)]$ of the excitation energy of the experimental 4_1^+ state to that of 2_1^+ state. In the lead region the value is in between one and two, indicating that these nuclei are spherical. In heavy Ra and Th isotopes, the ratio changes from 2 to 3.3, which indicates that these nuclei exhibit vibrational to rotational nature as the valence neutron number increases. Figure 1(b) shows the experimental excitation energies of the 3_1^- states. It is

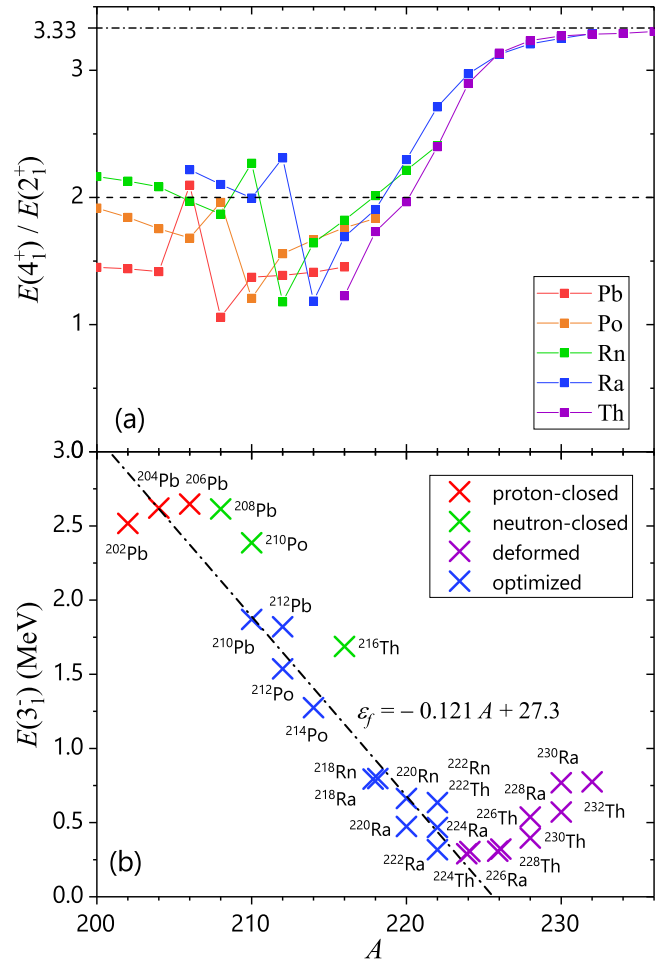

FIG. 1. (a) Ratio of the excitation energy of the 4_1^+ state to that of the 2_1^+ state, and (b) Excitation energies of the 3_1^- states for proton-closed (red), neutron-closed (green), deformed (violet), and other open-shell (blue) nuclei. The dot-dashed line indicates the single f-boson energy ε_f as a function of mass A. A more detailed discussion on the optimized parameters of the single f-boson energy ε_f is given in the text.

shown in the figure that there is a strong correlation between two quantities $[R_{4/2}$ and $E(3_1^-)]$. The deformation feature appears in the $A \geqslant 224$ region, whose nuclei are not treated in the present paper. As for the Coriolis coupling strength, an optimum choice is $\alpha = -0.02$ MeV throughout all the nuclei considered.

The electric octupole ($E3$) transition operator is simply given as

$$O_\mu = e_f\left(f_\mu^{(3)\dagger} - \tilde{f}_\mu^{(3)}\right), \tag{10}$$

where e_f represents the effective charge of the collective f boson. Here it is assumed that the contributions to $E3$ transition probabilities from valence nucleons are small, compared with the collective contributions. The reduced transition probabilities are then given by

$$B(E3; (I_k; J)_f \to I'_{k'}) = e_f^2\, \delta_{I,I'}\delta_{k,k'}. \tag{11}$$

TABLE I. Experimental $B(E3)$ values in units of W.u. Excitation energies (Exc.) are given in units of MeV. The Weisskopf unit for the electric octupole transition is given as $B_{\rm sp}(E3) = 5.940 \times 10^{-2} A^2$ in units of $e^2{\rm fm}^6$ [2]. In the last column type of each electric octupole transition is given. Ambiguous type is enclosed in parentheses.

	J^π	Exc.	I^π	Exc.	$B(E3; J^\pi \to I^\pi)$		Type
^{206}Pb	3^-	2.648	0^+	0	36 (2)	[5,35]	collective
	7^-	2.200	4^+	1.998	0.28 (3)	[35]	noncollective
	7^-	2.200	4^+	1.684	0.361 (8)	[36]	noncollective
	12^+	4.027	9^-	2.658	0.137 (12)	[35]	noncollective
^{208}Pb	3^-	2.615	0^+	0	34.0 (5)	[3,4,37]	collective
^{210}Pb	3^-	1.870	0^+	0	26 (6)	[7,38]	collective
	3^-	2.828	0^+	0	14 (4)	[7,38]	(collective)
	11^-	2.512	8^+	1.278	21 (2)	[39]	(collective)
^{214}Rn	13^-	2.676	10^+	1.928	44 (8)	[40]	collective
^{212}At	18^+	2.250	15^-	1.605	24 (1)	[41] [a]	collective
	22^-	3.506	19^+	2.264	29 (9)	[41,42]	collective
	25^-	4.772	22^+	4.547	26.8 (14)	[41–43]	collective
^{214}Fr	11^+	0.638	8^-	0.122	10 (4)	[44,45]	(noncollective)
	14^-	1.661	11^+	0.638	25 (5)	[44,45]	collective

[a]Nuclear Data Sheets [42] is not consistent with the original paper.

As shown in Table I, large $B(E3)$ values of the ground 0^+ states to the 3^-_1 states are measured with good accuracy for ^{206}Pb [5,6], ^{208}Pb [3,4], and ^{210}Pb [7], which demonstrates the collective nature of the 3^-_1 states.

III. NUMERICAL RESULTS

As noted in the formalism, the shell-model I^π_k state indicates $|I^\pi_k\rangle_{\rm SM}$, while $|I^\pi_k; J\rangle_f$ is referred to as the f-boson $J^{\pi'}$ state coupled with the shell-model I^π_k state. Here the f-boson state has the opposite parity π' to the parity π of the corresponding shell-model state.

In the following calculations it should be noted that in the case of ^{206,210}Pb and ^{210}Po the shell model configuration space involves only two-particle (hole) configurations. However, in the case of ^{212,214}Po and also Rn, At, and Fr isotopes the shell-model configuration space includes all particles in the valence shells.

Figure 2 shows the energy spectra of $_{82}$Pb isotopes (^{206,210}Pb). The ^{206}Pb nucleus consists of two valence neutron holes out of the doubly magic core of ^{208}Pb. The valence space consists of six neutron orbitals, $2p_{1/2}$, $2p_{3/2}$, $1f_{5/2}$, $1f_{7/2}$, $0h_{9/2}$, and $0i_{13/2}$. Thus, the lowest spin among all the negative parity states in the valence space is 2, and the 1^- states were out of the shell-model configurations. As shown in Fig. 2, the experimental negative-parity states with spin 2 and spin 3 cannot be described in the shell-model framework either. In fact, the shell-model 2^-_1 and 3^-_1 states are predicted at 5.735 MeV (not shown in the figure) and 4.660 MeV, respectively. Without any kinds of core-excitations, low-spin negative-parity states cannot be reproduced.

In the present framework, where collective octupole-phonon excitations are taken into account, the one-to-one correspondence between theory and experiment for all the negative-parity states with spin $I \leqslant 3$ is well retained with the single f-boson energy as $\varepsilon_f = 2.648$ MeV. As shown in Table I, the experimental $B(E3)$ value from the 7^-_1 state to the 4^+_1 state, and that from the 12^+_1 state to the 9^-_1 state, are both one order of magnitude smaller than the single-particle estimate. In fact our calculation suggests that the 7^-_1 and 12^+_1 states correspond to the pure shell-model states, which are not related to the octupole-phonon excitations.

The ^{210}Pb nucleus consists of two valence neutrons out of the doubly magic core of ^{208}Pb. Experimental energy levels and electromagnetic properties of low-lying states were well reproduced in the previous shell-model study except for the 3^-_1 state observed at 1.870 MeV [21]. The most plausible explanation for the 3^-_1 state is that this state is the one-octupole-phonon excitation across the ^{208}Pb core on top of the ground 0^+ state. Recognizing that the 3^-_1 state is a collective octupole-phonon excited state (f-boson state), a number of f-boson states, not only on top of the ground state, but also on top of other shell-model states such as the 2^+_1 and 4^+_1 states, should be observed. The energy difference between such kind of an f-boson state and the corresponding shell-model state should be not so much different from the excitation energy of the 3^-_1 state if the f-boson state and the shell-model state are weakly coupled. It is indeed assumed weak in this work.

In the present framework, there should be an f-boson 3^- state coupled with the shell-model 2^+_1 state, which is predicted at 2.753 MeV with the configuration of $[|f\rangle \otimes |2^+_1\rangle]^{(3)}$. In the previous shell-model calculation [21], the 3^-_2 was predicted at 2.682 MeV with the configuration of $(\nu g_{9/2} j_{15/2})$. The experimental $B(E3)$ values in Table I, some of which were obtained by Coulomb excitations [7,38], are helpful to identify the structure of the experimental 3^-_2 state. It is shown from Eq. (11) that the theoretical $B(E3)$ value from the f-boson 3^- state to the shell-model 0^+_1 state should be exactly zero if the f-boson 3^- state is excited from the shell-model 2^+_1 state. Taking into account the above, we have the following assumption for the experimental 3^-_1, 3^-_2, and 3^-_3

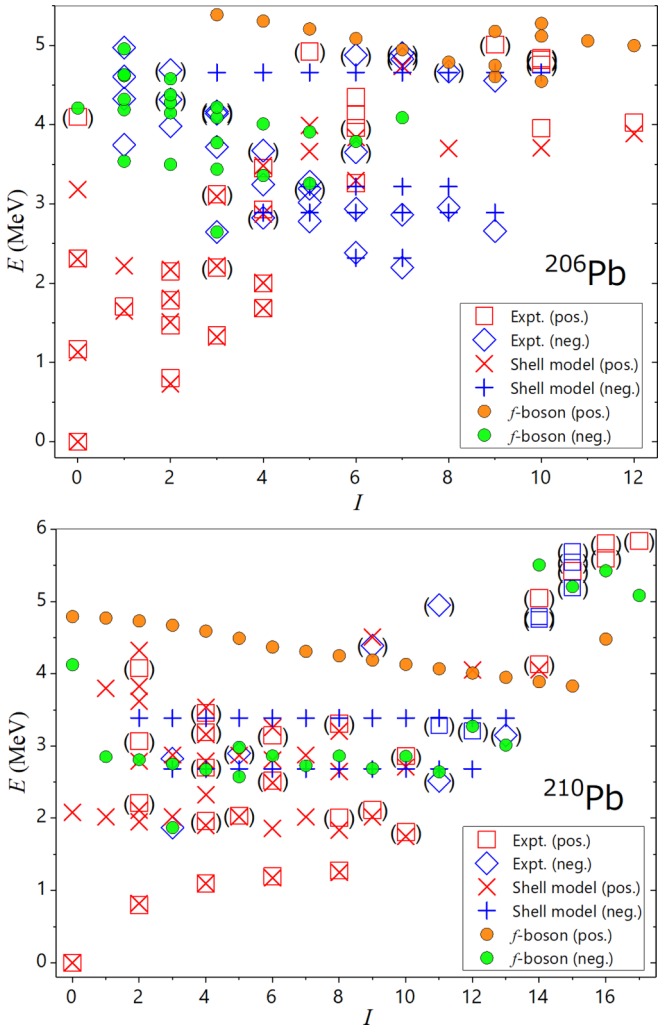

FIG. 2. Theoretical energy spectra including collective octupole-phonon (f-boson) excitations for Pb isotopes in comparison with experimental data [35,36,38,39]. As for the f-boson states indicated with filled circles, only the lowest state for each spin-parity is displayed unless the corresponding state is observed. The 1^-, 2^-, 3^-, 4^-, and 5^- states in ^{206}Pb and the 3^-_2 state and 5^-_2 state in ^{210}Pb are ones of the exceptions.

states as

$$|\widetilde{3^-_1}\rangle = \alpha|f \otimes 0^+_1\rangle + \beta|3^-_1\rangle_{\rm SM} \quad (12)$$

$$|\widetilde{3^-_2}\rangle = \beta|f \otimes 0^+_1\rangle - \alpha|3^-_1\rangle_{\rm SM} \quad (13)$$

$$|\widetilde{3^-_3}\rangle = |[f \otimes 2^+_1]^{(3)}\rangle, \quad (14)$$

where $\alpha^2 + \beta^2 = 1$. Here the coefficients α and β may be calculated through the octupole-octupole interaction between the valence nucleons and the octupole phonon. In this case a sum rule is obtained through Eq. (11), $B(E3; 3^-_1 \to 0^+_1) + B(E3; 3^-_2 \to 0^+_1) = e^2_f$.

Another possibility is that the experimental 3^-_1 and 3^-_2 states arise from two different kinds of collective-octupole modes with respect to neutron and proton degrees of freedom, namely f_ν and f_π. In fact there should be two kinds of excitations expressed as $|f_1\rangle = \alpha|f_\nu\rangle + \beta|f_\pi\rangle$ and $|f_2\rangle = \beta|f_\nu\rangle - \alpha|f_\pi\rangle$ where $\alpha^2 + \beta^2 = 1$. However, this possibility is low, considering the fact that in ^{208}Pb the 3^-_1 state appears at 2.615 MeV, but the 3^-_2 state appears at 4.051 MeV, which is rather high in energy. In order to avoid the complexity, this possibility is not discussed further, but left as a future problem. In this paper only one kind of collective mode characterized by the first 3^- state is assumed.

Figure 3 shows the energy spectra of $_{84}$Po isotopes (^{210,212,214}Po). The ^{210}Po nucleus consists of two valence protons in the shell model. In the previous shell-model study [20], the experimental 3^-_1, (11^-_2), (12^-_1), 13^-_1, and 14^-_1 states and some 5^-, 6^-, and 7^- states were not reproduced. Adopting the excitation energy of the experimental 3^-_1 state as the single f-boson energy ε_f, all the experimental 5^-, 6^-, 7^-, and 11^- states are well reproduced except for the 5^-_1 state. The 5^-_1 state is supposed to have nature of a single-particle excitation across the core. Here it should be noted in mind that the experimental 5^-_1 state appearing at 3.198 MeV in ^{208}Pb. In contrast neither of the (12^-_1), 13^-_1, and 14^-_1 states are reproduced in the present framework. The f-boson 12^-, 13^-, and 14^- states are actually predicted more than 6 MeV higher in energy (not shown in the figure). These high-spin states seemingly have nature of single-particle excitations across the core on top of the pure shell-model states. For example, the 14^-_1 state is so constructed that the lowest 6^- particle-hole excitation across the core is coupled to the shell-model 8^+_1 state. The excitation energy of 6^- state in ^{208}Pb is 3.920 MeV. Therefore 4^-, 5^-, and 6^- one particle-one hole excitations are necessary for the description of the (12^-_1), 13^-_1, and 14^-_1 states, respectively.

For ^{212}Po, the negative-parity states with spins lower than 11 were reported by the EUROBALL collaboration [46,47]. The authors assumed that the (3^-_1), (5^-_1), (7^-_1), and (9^-_1) states mainly consist of one-octupole-phonon excitations based on an analogy of the shell-model study in ^{148}Gd [49]. In the previous shell-model calculations of ^{212}Po [21], all the negative-parity states were predicted high in energy compared with experiment. The shell-model 3^-_1 state was calculated at 2.430 MeV whereas the experimental 3^-_1 state is observed at 1.537 MeV. Adopting the excitation energy of the experimental 3^-_1 state as the single f-boson energy ε_f, not only the experimental (3^-_1), (5^-_1), (7^-_1), and (9^-_1) states, but also the (11^-_1) and (13^-_1) states are well reproduced.

In contrast it is impossible in the present study to reproduce the low-lying (4^-), (6^-), and (8^-) states just below the excitation of 2 MeV. Based on enhanced $E1$ transition probabilities, the EUROBALL group pointed out that these states may have $\alpha + ^{208}$Pb cluster structure, which are out of the present framework. A further study is necessary to draw a definite conclusion.

Concerning the ^{214}Po nucleus in Fig. 3, the experimental 1^-_1, (2^-_1), and (3^-_1) states were out of the shell-model framework [21]. In the present calculation with the f boson they are reproduced with the single f-boson energy as $\varepsilon_f = 1.275$ MeV, where the excitation energy of the experimental 3^-_1 state is adopted. The first f-boson 2^- and 1^- states, and the second 1^- state are coupled with the shell-model 2^+_1, 2^+_1, and 4^+_1 states, respectively.

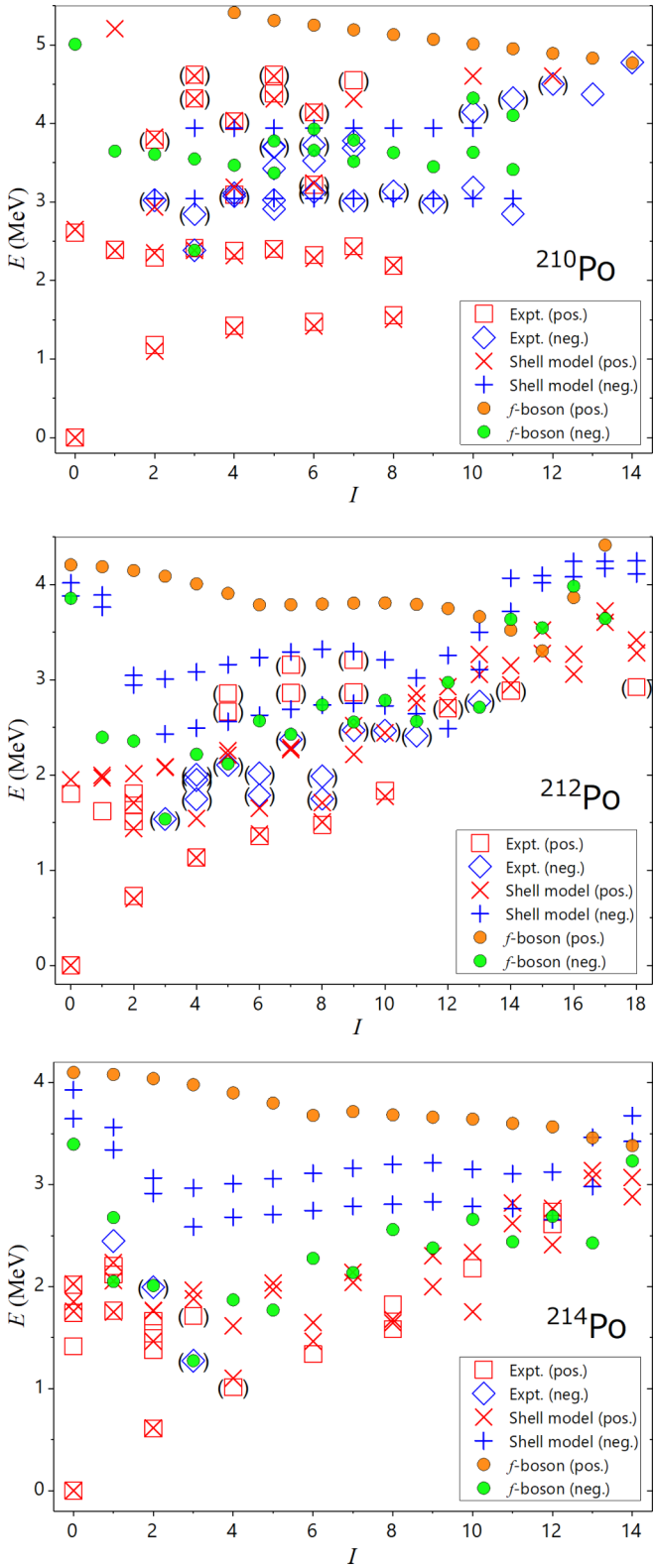

FIG. 3. The same as Fig. 2, but for Po isotopes. The experimental data are taken from Refs. [36,38,42,44,46–48].

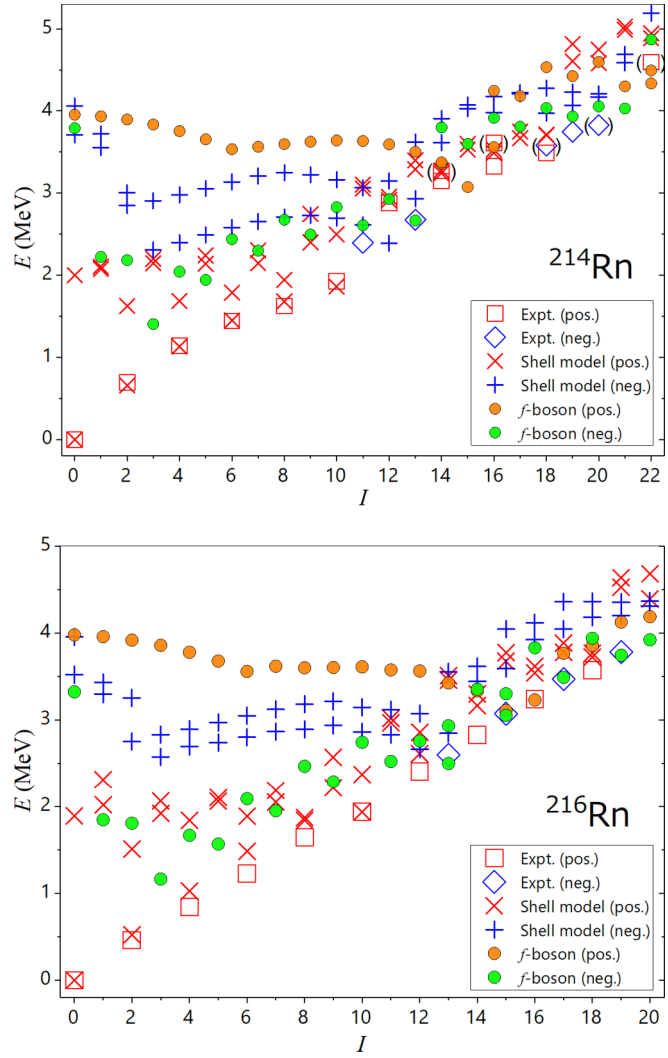

FIG. 4. The same as Fig. 2, but for Rn isotopes. The experimental data are taken from Refs. [36,44,50].

Figure 4 shows the energy spectra of $_{86}$Rn isotopes (^{214,216}Rn). In ^{214}Rn and ^{216}Rn, 3^- states have not been observed to date. In ^{214}Rn a low-lying state with unassigned spin and parity is observed at 1.331 MeV (not shown in the figure), which is rather high in energy for the positive-parity states predicted in the previous shell-model framework. Thus this state is presumed as the collective octupole-phonon excited state. As for the single f-boson energies, linearly optimized values of $\varepsilon_f = 1.406$ MeV and 1.164 MeV in Eq. (9) are adopted for ^{214}Rn and ^{216}Rn, respectively. The shell-model 11_1^-, 13_1^-, 19_1^-, 20_1^-, and 22_1^+ states of ^{214}Rn were calculated [21] slightly high in energy in comparison with experiment. In the present framework with f boson, the experimental 13_1^-, 19_1^-, (20_1^-), and 22_1^+ states are preferably reproduced. The experimental $B(E3; 13_1^- \rightarrow 10_1^+)$ value of 44(8) W.u. shown in Table I is considerably larger than the single-particle estimate. Therefore it is inferred that the experimental 13_1^- state mainly consists of the f-boson state, $[|f\rangle \otimes |10_1^+\rangle]^{(13)}$.

The experimental $(18)^-$ state at 3.579 MeV with ambiguity in spin cannot be well reproduced both in the previous shell-model calculation and the present framework with f boson. A two-octupole-phonon state on top of the shell-model 12_1^- state at 2.389 MeV may correspond to the $(18)^-$ state.

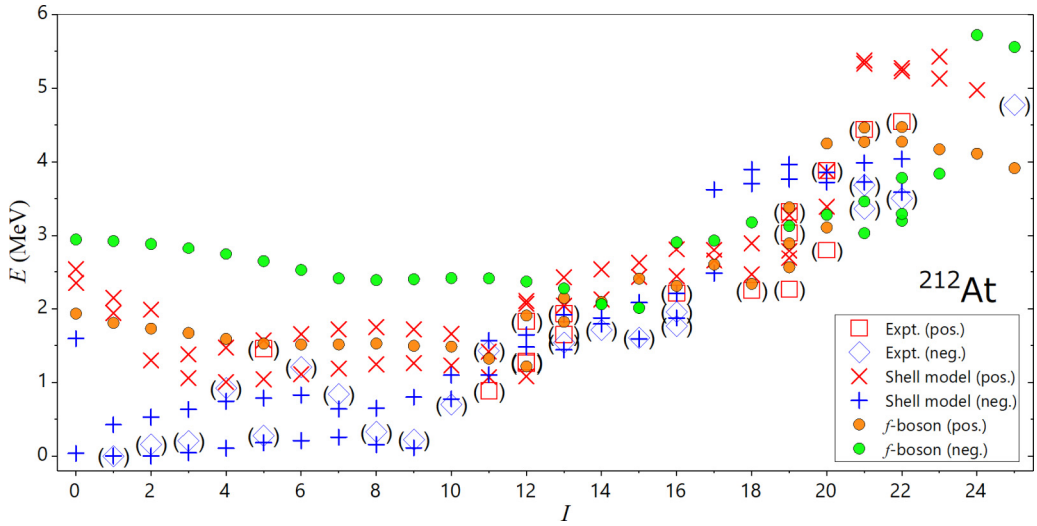

FIG. 5. The same as Fig. 2, but for ^{212}At. The experimental data are taken from Refs. [36,42].

In ^{216}Rn, the 13^-_1, 15^-_1, 17^-_1, and 19^-_1 states were observed through the ^{208}Pb (^{18}O, $2\alpha 2n$) reaction [8]. These negative-parity states and the 16^+_1 state at 3.238 MeV are well reproduced in the present framework. The first f-boson 13^-, 15^-, 17^-, 19^-, and 16^+ states are so constructed by the octupole-phonon excitation on top of the shell-model 10^+_1, 12^+_1, 14^+_1, 16^+_1, and 13^-_1 states, respectively.

Figure 5 shows the energy spectrum of $^{212}_{85}$At. One of the almost degenerate (12^+_1) and (12^+_2) states (at 1.262 MeV and 1.283 MeV), and the (13^+_1) state are well reproduced in the present framework. As shown in Table I, $B(E3)$ values larger than 20 W.u. are measured for the (18^+_1), (22^-_1), and (25^-_1) states, which demonstrates that these states are mainly constructed by the collective octupole-phonon excitations. In the present framework with $\varepsilon_f = 1.648$ MeV, some f-boson 18^+ and 22^- states appear close to the experimental (18^+_1) and (22^-_1) states in energy. In contrast, the (25^-_1) state cannot be reproduced in the present framework. The (25^-_1) state with ambiguity of spin-parity can be regarded as a two-octupole-phonon state on top of the one-octupole-phonon 22^+_1 state predicted above 4.273 MeV. Spin and parity of the (25^-_1) state should be confirmed in experiment.

Figure 6 shows the energy spectrum of $^{214}_{87}$Fr. Low-lying (11^+) and (12^+) states are well reproduced. In the present framework, the (11^+_1) state, where $B(E3; 11^+ \to 8^-) = 10(4)$ W.u. is observed, preferably corresponds to the shell-model 11^+_1 state. The neutron configuration of the shell-model 11^+_1 state consists of the $(\nu j_{15/2})$ orbital while that of the 8^-_1 state consists of the $(\nu g_{9/2})$ orbital. The experimental $B(E3)$ value is not so different from the single-particle estimate of $B(E3; 0j_{15/2} \to 1g_{9/2}) = 4.84$ W.u., assuming the neutron effective charge of $e_\nu = e$. Another possibility is to assume that the experimental 11^+_1 and 11^+_2 states are mixtures of the shell-model 11^+_1 state and the first f-boson 11^+ state as

$$|\widetilde{11^+_1}\rangle = \alpha|f \otimes 8^-_1\rangle + \beta|11^+_1\rangle_{\rm SM} \quad (15)$$

$$|\widetilde{11^+_2}\rangle = \beta|f \otimes 8^-_1\rangle - \alpha|11^+_1\rangle_{\rm SM}, \quad (16)$$

where $\alpha^2 + \beta^2 = 1$.

As shown in Table I, the value of $B(E3; 14^- \to 11^+) = 25(5)$ W.u. is reasonably large so that the (14^-_1) state mainly consists of f-boson states. In the present framework, the lowest two f-boson 14^- states and the shell-model 14^-_1 state are calculated approximately at the same energy of the experimental (14^-_1) state. However, the higher f-boson 14^- state is excluded since this state is constructed by an octupole-phonon excitation on top of the shell-model 12^+_1 state and then it cannot contribute to the $E3$ transition (see the discussion on the 3^-_2 state of ^{210}Pb). In contrast, the lower f-boson 14^- state is constructed on the shell-model 11^+_1 state, and then cause a large $E3$ transition to the shell-model 11^+_1 state. In conclusion, it is inferred that the (14^-_1) state is a mixture of the first f-boson 14^- state coupled with the shell-model 11^+_1, and the shell-model 14^-_1 state.

Through the present study, it is found that, among the experimental states whose $B(E3)$ values were measured, the

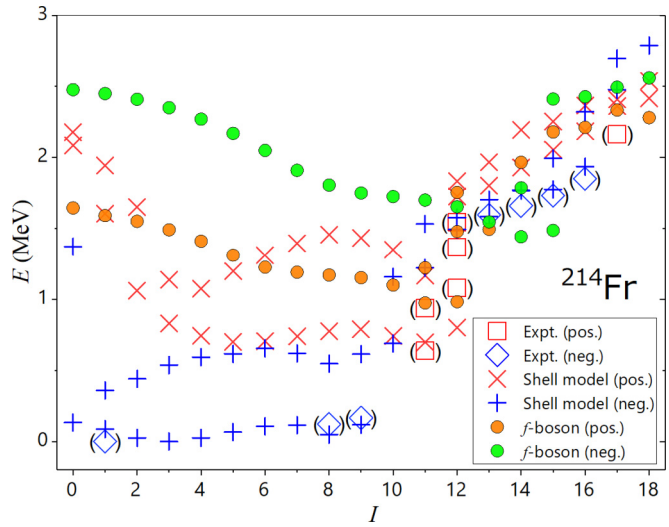

FIG. 6. The same as Fig. 2, but for ^{214}Fr. The experimental data are taken from Refs. [36,44].

3_1^- state of ^{206}Pb, the 3_1^- state of ^{208}Pb, the 3_1^- state of ^{210}Pb, the 13_1^- state of ^{214}Rn, the 18_1^+, 22_1^-, and 25_1^- states of ^{212}At, and the 14_1^- state of ^{214}Fr are mainly constructed by the collective octupole-phonon excitations. Using these experimental $B(E3)$ values, the effective charge of the collective f bosons is evaluated as

$$e_f^2 = (8.1 \pm 0.7) \times 10^4\ e^2\mathrm{fm}^6, \tag{17}$$

which corresponds to 31 ± 2.7 W.u. for the $B(E3; 3^- \to 0^+)$ transition with $A = 208$.

IV. SUMMARY

A model is proposed for the octupole vibrational states based on the nuclear shell model. In this model, a one-octupole-phonon representing the collective octupole vibration across the magic core is introduced on the microscopically calculated shell-model states. The model is applied to various nuclei around ^{208}Pb nucleus. Both pure shell-model states and octupole vibrational states are well reproduced. The type of each electric octupole transition is classified by either collective or noncollective nature. The electric octupole transition probabilities between the octupole vibrational states and the pure shell-model states are consistent with the simple estimate in Eq. (11). The effective charge for the f boson is obtained in comparison with the experimental data.

In this work we have introduced only one-octupole-phonons. There is some indication of two-octupole-phonon states. For instance in ^{214}Rn, a two-octupole-phonon state coupled with the shell-model 12_1^- state may correspond to the $(18)_1^-$ state. Two-phonon states should be included in the future. Also we need to introduce other high angular momentum excitations such as 5^- and 4^-, which have excitation energies of 3.197 and 3.475 MeV in ^{208}Pb. In this work we have only considered the Coriolis coupling between the shell-model states and the octupole phonon states. The model needs to be expanded by introducing other effective interactions that mix both the pure shell-model states and the f-boson states coupled with the shell-model states.

ACKNOWLEDGMENT

This work was supported by Grant-in-Aid for Scientific Research (C) (Grants No. 16K05341 and No. 17K05450) from Japan Society for the Promotion of Science (JSPS).

[1] A. Bohr and B. R. Mottelson, *Nuclear Structure*, Vol. II (Benjamin, New York, 1975).
[2] P. Ring and P. Schuck, *The Nuclear Many-Body Problem* (Springer Science & Business Media, Berlin, 2004).
[3] D. Goutte, J. B. Bellicard, J. M. Cavedon, B. Frois, M. Huet, P. Leconte, P. X. Ho, S. Platchkov, J. Heisenberg, J. Lichtenstadt, C. N. Papanicolas, and I. Sick, Phys. Rev. Lett. **45**, 1618 (1980).
[4] R. H. Spear, W. J. Vermeer, M. T. Esat, J. A. Kuehner, A. M. Baxter, and S. Hinds, Phys. Lett. B **128**, 29 (1983).
[5] J. F. Ziegler and G. A. Peterson, Phys. Rev. **165**, 1337 (1968).
[6] D. J. Horen, R. L. Auble, J. R. Beene, F. E. Bertrand, M. L. Halbert, G. R. Satchler, M. Thoennessen, R. L. Varner, V. R. Brown, P. L. Anthony, and V. A. Madsen, Phys. Rev. C **44**, 128 (1991).
[7] C. Ellegaard, P. D. Barnes, E. R. Flynn, and G. J. Igo, Nucl. Phys. A **162**, 1 (1971).
[8] M. E. Debray, J. Davidson, M. Davidson, A. J. Kreiner, M. A. Cardona, D. Hojman, D. R. Napoli, S. Lenzi, G. de Angelis, D. Bazzacco, S. Lunardi, M. DePoli, C. Rossi-Alvarez, A. Gadea, N. Medina, and C. A. Ur, Phys. Rev. C **73**, 024314 (2006).
[9] I. Hamamoto, Nucl. Phys. A **155**, 362 (1970).
[10] T. Aumann, P. F. Bortignon, and H. Emling, Annu. Rev. Nucl. Part. Sci. **48**, 351 (1998).
[11] V. Y. Ponomarev and P. von Neumann-Cosel, Phys. Rev. Lett. **82**, 501 (1999).
[12] B. A. Brown, Phys. Rev. Lett. **85**, 5300 (2000).
[13] B. D. Valnion, V. Y. Ponomarev, Y. Eisermann, A. Gollwitzer, R. Hertenberger, A. Metz, P. Schiemenz, and G. Graw, Phys. Rev. C **63**, 024318 (2001).
[14] E. Caurier, M. Rejmund, and H. Grawe, Phys. Rev. C **67**, 054310 (2003).
[15] A. Heusler, R. V. Jolos, and P. von Brentano, Phys. At. Nucl. **76**, 807 (2013).
[16] J. M. Yao and K. Hagino, Phys. Rev. C **94**, 011303 (2016).
[17] A. Heusler, R. V. Jolos, T. Faestermann, R. Hertenberger, H.-F. Wirth, and P. von Brentano, Phys. Rev. C **93**, 054321 (2016).
[18] E. Teruya, N. Yoshinaga, K. Higashiyama, and A. Odahara, Phys. Rev. C **92**, 034320 (2015).
[19] E. Teruya, N. Yoshinaga, K. Higashiyama, H. Nishibata, A. Odahara, and T. Shimoda, Phys. Rev. C **94**, 014317 (2016).
[20] E. Teruya, K. Higashiyama, and N. Yoshinaga, Phys. Rev. C **93**, 064327 (2016).
[21] K. Yanase, E. Teruya, K. Higashiyama, and N. Yoshinaga, Phys. Rev. C **98**, 014308 (2018).
[22] J. Engel, M. Bender, J. Dobaczewski, J. H. de Jesus, and P. Olbratowski, Phys. Rev. C **68**, 025501 (2003).
[23] O. P. Sushkov, V. V. Flambaum, and I. B. Khriplovich, Zh. Eksp. Teor. Fiz. **87**, 1521 (1984).
[24] N. Auerbach, V. F. Dmitriev, V. V. Flambaum, A. Lisetskiy, R. A. Sen'kov, and V. G. Zelevinsky, Phys. Rev. C **74**, 025502 (2006).
[25] N. Auerbach, V. Dmitriev, V. Flambaum, A. Lisetskiy, R. Sen'kov, and V. Zelevinsky, Phys. At. Nucl. **70**, 1654 (2007).
[26] N. Yamanaka and E. Hiyama, Phys. Rev. C **91**, 054005 (2015).
[27] N. Yamanaka and E. Hiyama, J. High Energy Phys. 02 (2016) 067.
[28] N. Yamanaka, T. Yamada, E. Hiyama, and Y. Funaki, Phys. Rev. C **95**, 065503 (2017).
[29] N. Yoshinaga, K. Higashiyama, R. Arai, and E. Teruya, Phys. Rev. C **87**, 044332 (2013).
[30] E. Teruya, N. Yoshinaga, K. Higashiyama, and K. Asahi, Phys. Rev. C **96**, 015501 (2017).
[31] N. Yamanaka, B. K. Sahoo, N. Yoshinaga, T. Sato, K. Asahi, and B. P. Das, Eur. Phys. J. A **53**, 54 (2017).
[32] N. Yoshinaga, K. Higashiyama, and R. Arai, Prog. Theor. Phys. **124**, 1115 (2010).
[33] N. Yoshinaga, K. Higashiyama, R. Arai, and E. Teruya, Phys. Rev. C **89**, 045501 (2014).

[34] K. Yanase, N. Yoshinaga, K. Higashiyama, and N. Yamanaka, arXiv:1805.00419.
[35] F. Kondev, Nucl. Data Sheets **109**, 1527 (2008).
[36] Evaluated Nuclear Structure Data File (ENSDF), http://www.nndc.bnl.gov/ensdf/
[37] M. J. Martin, Nucl. Data Sheets **108**, 1583 (2007).
[38] M. S. Basunia, Nucl. Data Sheets **121**, 561 (2014).
[39] R. Broda, L. W. Iskra, R. V. F. Janssens, B. A. Brown, B. Fornal, J. Wrzesiński, N. Cieplicka-Oryńczak, M. P. Carpenter, C. J. Chiara, C. R. Hoffman, F. G. Kondev, G. J. Lane, T. Lauritsen, Z. Podolyák, D. Seweryniak, W. B. Walters, and S. Zhu, Phys. Rev. C **98**, 024324 (2018).
[40] G. D. Dracoulis, A. P. Byrne, A. E. Stuchbery, R. A. Bark, and A. R. Poletti, Nucl. Phys. A **467**, 305 (1987).
[41] S. Bayer, A. Byrne, G. Dracoulis, A. Baxter, T. Kibedi, F. Kondev, S. Mullins, and T. McGoram, Nucl. Phys. A **650**, 3 (1999).
[42] E. Browne, Nucl. Data Sheets **104**, 427 (2005).
[43] A. P. Byrne, S. Bayer, G. D. Dracoulis, and T. Kibédi, Phys. Rev. Lett. **80**, 2077 (1998).
[44] S.-C. Wu, Nucl. Data Sheets **110**, 681 (2009).
[45] A. Byrne, G. Lane, G. Dracoulis, B. Fabricius, T. Kibédi, A. Stuchbery, A. Baxter, and K. Schiffer, Nucl. Phys. A **567**, 445 (1994).
[46] A. Astier, P. Petkov, M.-G. Porquet, D. S. Delion, and P. Schuck, Phys. Rev. Lett. **104**, 042701 (2010).
[47] A. Astier, P. Petkov, M.-G. Porquet, D. S. Delion, and P. Schuck, Eur. Phys. J. A **46**, 165 (2010).
[48] A. Astier and M.-G. Porquet, Phys. Rev. C **83**, 014311 (2011).
[49] M. Piiparinen, P. Kleinheinz, S. Lunardi, M. Ogawa, G. de Angelis, F. Soramel, W. Meczynski, and J. Blomqvist, Z. Phys. A: At. Nucl. **337**, 387 (1990).
[50] S.-C. Wu, Nucl. Data Sheets **108**, 1057 (2007).